Calcolo (2012) 49:1–19
DOI 10.1007/s10092-011-0041-1

Applications of the pseudo residual-free bubbles to the stabilization of convection-diffusion-reaction problems

Ali Sendur · Ali I. Nesliturk

Received: 13 November 2010 / Accepted: 22 March 2011 / Published online: 8 April 2011

Abstract It is known that the enrichment of the polynomial finite element space of degree 1 by bubble functions results in a stabilized scheme of the SUPG-type for the convection-diffusion-reaction problems. In particular, the residual-free bubbles (RFB) can assure stabilized methods, but they are usually difficult to compute, unless the configuration is simple. Therefore it is important to devise numerical algorithms that provide cheap approximations to the RFB functions, contributing a good stabilizing effect to the numerical method overall. Here we propose a stabilization technique based on the RFB method and particularly designed to treat the most interesting case of small diffusion. We replace the RFB functions by their cheap, yet efficient approximations which retain the same qualitative behavior. The approximate bubbles are computed on a suitable sub-grid, the choice of whose nodes are critical and determined by minimizing the residual of a local problem with respect to L_1 norm. The resulting numerical method has similar stability features with the RFB method for the whole range of problem parameters. This fact is also confirmed by numerical experiments. We also note that the location of the sub-grid nodes suggested by the strategy herein coincides with the one in Brezzi et al. (Math. Models Methods Appl. Sci. 13:445–461, 2003).

Keywords Stabilized finite elements · Residual-free bubbles · Augmented space

Mathematics Subject Classification (2000) 65L10 · 65L11 · 65L60

A. Sendur · A.I. Nesliturk (✉)
Department of Mathematics, Izmir Institute of Technology, 35430 Izmir, Turkey
e-mail: alinesliturk@iyte.edu.tr

A. Sendur
e-mail: alisendur@iyte.edu.tr

1 Introduction

It is well known that the convection-diffusion-reaction problems may contain thin regions in which the solution varies abruptly. The plain Galerkin method may not work for such problems on reasonable discretizations, producing unphysical oscillations. The SUPG method, and its variants, are among the most popular approaches to overcome that difficulty, which are based on augmenting the variational formulation by mesh-dependent terms in order to gain control over the derivatives of the solution [10, 12, 16]. The great advantage of this approach is not only its generality, but also its error analysis can be performed in many cases of interest. Nevertheless, the need for the proper choice of stabilizing parameter is considered as a major drawback of the method.

Another approach consists of enriching the finite element spaces by bubble functions. The relationship between the use of bubble functions and stabilized methods was also studied in [1–3]. It turns out that, to find a more suitable value for the stabilizing parameter in the SUPG method, it is crucial to use special type of functions, so called the residual-free bubbles (RFB), defined by a local problem posed inside each element. The RFB method also allows one to prove error bounds [6, 19] and can be generalized to a much wider variety of problems [5, 13]. However it requires solving a local differential equation which may not be easier than to solve the original one [14, 15].

Yet another way of stabilizing the Galerkin method is to stabilize by means of a suitable refinement around the layer so that, the stabilization is actually not needed anymore, like in the Shishkin meshes [11]. The drawback of these methodologies resides in that they require a priori knowledge of the layer locations.

Here, we will present a stabilization method for one-dimensional convection-diffusion-reaction problems, particularly designed to treat the most interesting case of small diffusion, but able to adapt from one regime to another continuously. It is based on the RFB method, in which, however, we replace the RFB functions by their cheap, yet efficient approximations, so called pseudo RFBs, which retain the same qualitative behavior as the RFBs. Similar approaches to obtain suitable approximations to the RFBs can be found in the literature [4, 7, 9, 17, 18]. The pseudo bubbles are chosen to be piecewise linear on a suitable sub-grid that, the position of whose nodes are determined by minimizing the residual of local differential problems with respect to L_1 norm. The recipe for spotting sub-grid points is simple and their location coincides with the one in [8]. The resulting numerical method has similar stability features to the RFB method for the whole range of problem parameters. This fact is confirmed by numerical experiments presented below.

The layout of the paper is as follows: We review the RFB method in Sect. 2. In Sect. 3, we discuss the explicit locations of sub-grid nodes on which we construct the pseudo bubble functions and describe the details of the numerical method proposed. Finally we perform the numerical tests in Sect. 4.

2 A review of RFB for boundary value problems

We will consider the following linear elliptic convection-diffusion-reaction problem in $I = (0, 1)$:

$$\mathcal{L}u = -\epsilon u'' + \beta u' + \sigma u = f(x) \quad \text{with } u(0) = u(1) = 0 \tag{1}$$

Let $0 = x_0 < x_1 < x_2 < \cdots < x_{N-1} < x_N = 1$ and $\mathcal{T}_h = \{K\}$ be a decomposition of I into subintervals $K = (x_{k-1}, x_k)$ where $k = 1, \ldots, N$. For the sake of simplicity, we shall assume that the decomposition is uniform, so that we can denote the length of the intervals in the subdivision by h. However, all our discussions will take place at the element level, and therefore, they will also be valid for quasi-uniform decompositions.

We assume that the diffusion coefficient ϵ is a positive constant, and that the convection field β and the reaction field σ are non-negative piecewise constants with respect to the decomposition $\mathcal{T}_h$. So, unless $\beta \equiv 0$ (pure reaction case), we can speak of inflow and outflow. When $\epsilon \ll |\beta|h + \sigma h^2$, the solution of the problem will have boundary layers for a generic f, that can be either only at the outflow, or at both ends of I, depending on the reciprocal values of $|\beta|h$ and σh^2. In these cases, the pure Galerkin method will typically fail, showing strong oscillations near the boundary layers, and some stabilization is needed.

Here we will consider stabilizations based on the augmented space idea which includes the RFB strategy, and it can be summarized as follows. We start by recalling the abstract variational formulation of problem (1): Find $u \in H_0^1(I)$ such that

$$a(u, v) = (f, v), \quad \forall v \in H_0^1(I) \tag{2}$$

where

$$a(u, v) = \epsilon \int_I u'v'\,dx + \int_I (\beta u)'v\,dx + \int_I \sigma uv\,dx \tag{3}$$

We now define V_h as a finite-dimensional space, which is a subspace of $H_0^1(I)$. Then the standard Galerkin finite element method reads: Find $u_h \in V_h$ such that

$$a(u_h, v_h) = (f, v_h), \quad \forall v_h \in V_h \tag{4}$$

Now, we decompose the space V_h such that $V_h = V_L \oplus V_B$, where V_L is the space of continuous piecewise linear polynomials and $V_B = \bigoplus_K B_K$ with $B_K = H_0^1(K)$ Then every $v_h \in V_h$ can be written in the form of $v_h = v_L + v_B$, where $v_L \in V_L$ and $v_B \in V_B$. We require the bubble component u_B of u_h to satisfy the original differential equations in K strongly, i.e.

$$\mathcal{L}u_B = -\mathcal{L}u_L + f \quad \text{in } K \tag{5}$$

subject to the boundary condition,

$$u_B = 0 \quad \text{on } \partial K. \tag{6}$$

By the classical static condensation procedure [8], the method used to compute an improved linear approximation due to the residual-free bubble effect reads: Find $u_h = u_L + u_B$ in V_h such that

$$a(u_L, v_L) + a(u_B, v_L) = (f, v_L), \quad \forall v_L \in V_L \tag{7}$$

The term $a(u_B, v_L)$ is responsible for the stabilization of the numerical method and the bubble component u_B should be computed before we solve (7) for its linear part. Recall u_B is identified by the linear part u_L and the source function f through (5)–(6), which may be as complicated as solving the original differential equation. Therefore, it is important to bring a simple recipe about to obtain a suitable approximation to the bubble component of the problem that provides a similar stabilizing effect into the numerical method. We discuss that approach in the following section. The discussion will take place in a typical element K, and therefore, we shall drop the index K in the notation unless it is necessary.

3 The choice of the sub-grid nodes

Let us define a sub-grid in a typical element $K = (x_{k-1}, x_k)$ by adding two points z_1 and z_2 with the property that

$$x_{k-1} < z_1 < z_2 < x_k \tag{8}$$

on which, we approximate the bubble functions. The shape of approximations, which is essentially related with the location of sub-grid points, is crucial to get a good stabilization effect on the numerical method. Therefore the choice of points in the sub-grid must be fulfilled in a special manner. That will be accomplished by a minimization process with respect to L_1 norm in the presence of layers.

Let us assume that f is a piecewise linear function with respect to the discretization. Then the residual in (5) becomes a linear function and it is reasonable to consider bubble functions B_i $(i = 1, 2)$ defined by

$$\mathcal{L}B_i = -\mathcal{L}\psi_i \quad \text{in } K, \qquad B_i = 0 \quad \text{on } \partial K,\ i = 1, 2 \tag{9}$$

where ψ_1, ψ_2 are the restrictions of the piecewise linear basis functions for V_L to K (Fig. 1). Further we define B_f,

$$\mathcal{L}B_f = f \quad \text{in } K, \qquad B_f = 0 \quad \text{on } \partial K \tag{10}$$

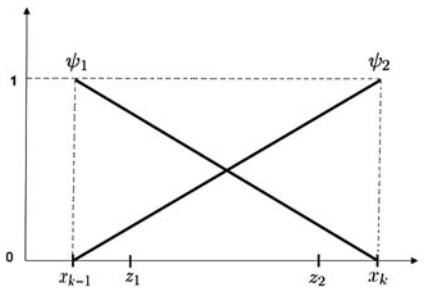

Fig. 1 The restrictions of piecewise linear basis functions to a typical element K

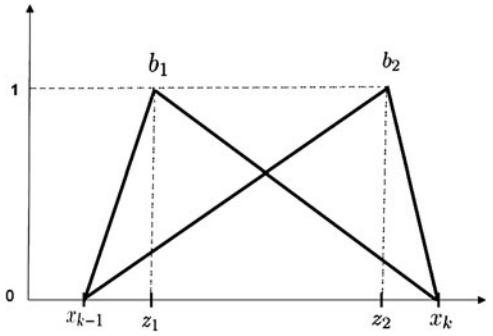

Fig. 2 Basis functions employed in the approximation of bubble functions

Now if

$$u_L|_K = u_L(x_{k-1})\psi_1 + u_L(x_k)\psi_2$$

then, we take

$$u_B|_K = u_L(x_{k-1})B_1 + u_L(x_k)B_2 + B_f \tag{11}$$

Thus

$$\begin{aligned}\mathcal{L}u_B &= u_L(x_{k-1})\mathcal{L}B_1 + u_L(x_k)\mathcal{L}B_2 + \mathcal{L}B_f \\ &= u_L(x_{k-1})(-\mathcal{L}\psi_1) + u_L(x_k)(-\mathcal{L}\psi_2) + f \\ &= -\mathcal{L}(u_L(x_{k-1})\psi_1 + u_L(x_k)\psi_2) + f = -\mathcal{L}u_L + f \quad \text{in } K\end{aligned}$$

That is, (5) is automatically satisfied with the present choice of bubble functions. Equation (9) is similar to the original problem (1) and may be difficult to solve. However, using the element geometry and the problem properties, it is possible to construct a cheap, yet efficient approximate bubbles, say B_i^*, over the sub-grid (8), having the same qualitative behavior with its continuous counterpart B_i $(i = 1, 2)$. The construction of such approximate bubble functions B_i^* is given in the following.

Let $B_i^*(x) = \alpha_i b_i(x)$ be the classical Galerkin approximation of B_i through (9), that is,

$$a(B_i^*, b_i)_K = (-\mathcal{L}\psi_i, b_i)_K, \quad i = 1, 2 \tag{12}$$

where b_i is a piecewise linear function with the following properties (Fig. 2);

$$b_i(x_{k-1}) = b_i(x_k) = 0, \qquad b_i(z_i) = 1, \quad i = 1, 2$$

Using integration by parts, the properties of bubble functions and the midpoint rule for quadratic terms that appears, we get explicit expressions for α_1 and α_2, separately:

$$\alpha_1 = \frac{(-\mathcal{L}\psi_1, b_1)_K}{\epsilon\|b_1'\|_K^2 + \sigma\|b_1\|_K^2} = \frac{3\beta + (\xi - 2h)\sigma}{2h(\frac{3\epsilon}{\xi(h-\xi)} + \sigma)} \tag{13}$$

and

$$\alpha_2 = \frac{(-\mathcal{L}\psi_2, b_2)_K}{\epsilon \|b_2'\|_K^2 + \sigma \|b_2\|_K^2} = -\frac{3\beta + (2h-\eta)\sigma}{2h(\frac{3\epsilon}{\eta(h-\eta)} + \sigma)} \tag{14}$$

Note that $\alpha_2 < 0$. Now it remains to choose z_i, so that the stabilizing effect of bubble function B_i is maintained in its discrete counterpart B_i^* $(i = 1, 2)$. The main criteria that we use to determine the locations of the sub-grid nodes is to minimize L_1 norm of the residual coming out from the bubble equation (9) in the critical case where a layer structure exists. In other words, we choose z_i such that

$$J_i = \int_K |\mathcal{L}B_i^* + \mathcal{L}\psi_i| \, dx, \quad i = 1, 2 \tag{15}$$

is minimum. That approach (15) were also used in [4]. Before we derive the explicit locations of sub-grid points that emerges from the criterion (15), let us make some general observations on their configuration. Set

$$\begin{aligned} &\xi = z_1 - x_{k-1}, \qquad \eta = x_k - z_2, \qquad \delta = z_2 - z_1 \\ &K_1 = [x_{k-1}, z_1], \qquad K_2 = [z_1, z_2], \qquad K_3 = [z_2, x_k] \end{aligned} \tag{16}$$

From (8) and (16), it is obvious that $\xi + \delta + \eta = h$. At the same time, we do not want δ to be too small, either, when compared with ξ and η. Therefore we take,

$$\delta \geq \min\{\xi, \eta\} \tag{17}$$

From the qualitative behavior of the problem (1), we always have $\eta \leq \xi$, which implies $\delta \geq \eta$. Hence η will always be the smallest of the three sub-lengths and, thus we have

$$\eta \leq h/3 \tag{18}$$

Now we are in a position to give the explicit description of sub-grid points for each type of problem regime.

3.1 Diffusion-dominated regime

In the present algorithm, the problem is assumed to be diffusion-dominated when $6\epsilon > \beta h + \sigma h^2/9$. In this regime, the stabilization is not needed, and a uniform sub-grid seems to be appropriate. Therefore we choose $\xi = \eta = \delta = h/3$.

3.2 Convection-dominated regime

In convection dominated case, we have a single exponential boundary layer at the outflow. Therefore it is enough to find an optimal location for z_2 only and place z_1 on an appropriate location with respect to the configuration of the problem. We assume that the problem is convection-dominated if $6\epsilon \leq \beta h + \sigma h^2/9$ with $3\beta \geq \sigma h$. The following lemma suggests an optimal position for z_2 by using (15).

Lemma 1 *In convection-dominated case, the point* $\eta_e = \frac{-3\beta+\sqrt{9\beta^2+24\epsilon\sigma}}{2\sigma}$ *minimizes the integral* (15) *for* $i = 2$.

Proof Following the lines of [4], it is possible to write the integral J_2 as follows:

$$J_2 = \int_K |-\epsilon B_2^{*\prime\prime}|\,dx + \int_K |\beta B_2^{*\prime} + \sigma B_2^* + \beta\psi_2{}' + \sigma\psi_2|\,dx \tag{19}$$

Let $g_2 = \beta B_2^{*\prime} + \sigma B_2^* + \beta\psi_2{}' + \sigma\psi_2$. Then, a direct calculation over K gives,

$$\begin{aligned}\int_K g_2\,dx &= \beta + \frac{\sigma h}{2}(\alpha_2+1) = \beta + \frac{\sigma h}{2}\left(1 - \frac{3\beta+(2h-\eta)\sigma}{2h(\frac{3\epsilon}{\eta(h-\eta)}+\sigma)}\right)\\ &= \frac{\beta[12\epsilon+\sigma\eta(h-\eta)]+\sigma[6\epsilon h+\sigma\eta^2(h-\eta)]}{12\epsilon+4\sigma\eta(h-\eta)}\end{aligned} \tag{20}$$

which is always positive. Now we split the element K by z_2 and investigate the sign of g_2 in each of these subdomains. In that direction, use $\sigma\eta \le \sigma\frac{h}{3} < \beta$ and $\alpha_2 < 0$, to get

$$\begin{aligned}g_2|_{K_3} &= -\alpha_2\frac{\beta}{\eta} - \alpha_2\frac{\sigma(x-x_k)}{\eta} + \frac{\beta}{h} + \frac{\sigma(x-x_{k-1})}{h}\\ &= -\frac{\alpha_2}{\eta}(\beta-\sigma(x_k-x)) + \frac{1}{h}(\beta+\sigma(x-x_{k-1}))\\ &\ge -\frac{\alpha_2}{\eta}(\beta-\sigma\eta) + \frac{1}{h}(\beta+\sigma(x-x_{k-1})) > 0\end{aligned}$$

Thus the second term on the right hand side of (19) attains its minimum if $g_2\,|_{K_1\cup K_2}$ is non-negative, too. That is,

$$\begin{aligned}g_2|_{K_1\cup K_2} &= \alpha_2\frac{\beta}{h-\eta} + \alpha_2\frac{\sigma(x-x_{k-1})}{h-\eta} + \frac{\beta}{h} + \frac{\sigma(x-x_{k-1})}{h}\\ &= (\beta+\sigma(x-x_{k-1}))\left(\frac{\alpha_2}{h-\eta}+\frac{1}{h}\right)\\ &= (\beta+\sigma(x-x_{k-1}))\frac{-\sigma\eta^2-3\beta\eta+6\epsilon}{2h(3\epsilon+\sigma\eta(h-\eta))}\end{aligned}$$

is positive, only if

$$\eta \le \frac{-3\beta+\sqrt{9\beta^2+24\epsilon\sigma}}{2\sigma} \tag{21}$$

On the other hand, the first term on the right hand side of (19) is a locally decreasing function of η, since

$$\int_K |-\epsilon B_2^{*\prime\prime}|\,dx = -\alpha_2\frac{\epsilon h}{\eta(h-\eta)}$$

and

$$\frac{d}{d\eta}\left(-\alpha_2\frac{\epsilon h}{\eta(h-\eta)}\right) = -\frac{\epsilon(h-2\eta)(3\beta+\sigma(2h-\eta))}{2\eta(h-\eta)(3\epsilon+\sigma\eta(h-\eta))} < 0 \tag{22}$$

This fact together with (21) determines an optimal value for η. □

Remark 1 The value of η_e coincides with the one suggested in [8].

Remark 2 The value of α_2 at η_e is simply equal to $\frac{\eta_e}{h} - 1$.

The choice of other lengths δ and ξ should be consistent with the physics of the problem. Thus we take $\eta = \eta_e$, $\delta = \eta$ and ξ is chosen accordingly ($\xi = h - 2\eta$).

3.3 Reaction-dominated regime

In reaction-dominated case, we have two parabolic boundary layers at both ends and the location of both sub-grid points z_1 and z_2 should be chosen in such a way that approximate bubble functions mimic the exact ones. Thus we spot the position of z_2 from Lemma 1 and it remains to find a proper location for z_1, which can be accomplished by minimizing the integral

$$J_1 = \int_K |\mathcal{L}B_1^* + \mathcal{L}\psi_1|\,dx \tag{23}$$

Before we find an optimal position for z_1, we need the following intermediate result. Note that the problem is assumed to be reaction-dominated if $6\epsilon \le \beta h + \sigma h^2/9$ and $3\beta < \sigma h$.

Lemma 2 *Let α_1 be as in (13). In reaction dominated regime we have*

$$\frac{\xi}{2h} - 1 < \alpha_1 < 0$$

Proof The upper estimate can easily be obtained by using the fact that

$$3\beta + (\xi - 2h)\sigma < \sigma h + (\xi - 2h)\sigma = \sigma(\xi - h) < 0$$

To show the lower bound, observe that,

$$\begin{aligned}\alpha_1 + 1 &= \frac{3\beta + (\xi-2h)\sigma}{2h(\frac{3\epsilon}{\xi(h-\xi)} + \sigma)} + 1 = \frac{6\epsilon h + \xi(h-\xi)(3\beta+\sigma\xi)}{6\epsilon h + 2\sigma\xi h(h-\xi)} \\ &> \frac{6\epsilon h + \sigma\xi^2(h-\xi)}{6\epsilon h + 2\sigma\xi h(h-\xi)} > \frac{\xi(6\epsilon + \sigma\xi(h-\xi))}{2h(3\epsilon+\sigma\xi(h-\xi))} > \frac{\xi}{2h}\end{aligned}$$

□

The following lemma suggests an optimal position for z_1.

Lemma 3 *In reaction-dominated case, the point $\xi_e = \frac{3\beta+\sqrt{9\beta^2+24\epsilon\sigma}}{2\sigma}$ minimizes the integral (23).*

Proof It is possible to write the integral J_1 as follows:

$$J_1 = \int_K |-\epsilon B_1^{*\prime\prime}|\,dx + \int_K |\beta B_1^{*\prime} + \sigma B_1^* + \beta {\psi_1}' + \sigma \psi_1|\,dx \tag{24}$$

Let $g_1 = \beta B_1^{*\prime} + \sigma B_1^* + \beta {\psi_1}' + \sigma \psi_1$. Without loss of generality, assume $\xi > \frac{2\beta}{\sigma}$. Then we have

$$\begin{aligned}\int_K g_1\,dx &= -\beta + \frac{\sigma h}{2}(\alpha_1 + 1) = -\beta + \frac{\sigma h}{2}\left(\frac{3\beta + (\xi - 2h)\sigma}{2h(\frac{3\epsilon}{\xi(h-\xi)} + \sigma)} + 1\right)\\ &= \frac{6\epsilon(\sigma h - 2\beta) + \sigma\xi(h-\xi)(\sigma\xi - \beta)}{4(3\epsilon + \sigma\xi(h-\xi))} > 0\end{aligned} \tag{25}$$

Now split K into two subregions by z_1 and calculate the integral of g_1 over each of these sub-domains:

$$\begin{aligned}\int_{K_1} g_1\,dx &= \alpha_1\beta + \alpha_1\frac{\sigma\xi}{2} - \beta\frac{\xi}{h} - \frac{\sigma\xi}{2h}(\xi - 2h)\\ &= \beta\left(\alpha_1 - \frac{\xi}{h}\right) + \sigma\xi\left(\frac{\alpha_1}{2} - \frac{\xi}{2h} + 1\right)\\ &\geq \beta\left(\alpha_1 - \frac{\xi}{h}\right) + 2\beta\left(\frac{\alpha_1}{2} - \frac{\xi}{2h} + 1\right) = 2\beta\left(\alpha_1 - \frac{\xi}{h} + 1\right)\end{aligned} \tag{26}$$

where we have used Lemma 2. Further we have

$$\int_{K_2\cup K_3} g_1\,dx = \left(\sigma\frac{h-\xi}{2} - \beta\right)\left(\alpha_1 - \frac{\xi}{h} + 1\right) \tag{27}$$

The common factor of the last terms in (26)–(27) can be rewritten as

$$\alpha_1 - \frac{\xi}{h} + 1 = \frac{3\beta + (\xi - 2h)\sigma}{2h(\frac{3\epsilon}{\xi(h-\xi)} + \sigma)} - \frac{\xi}{h} + 1 = \frac{(h-\xi)(-\sigma\xi^2 + 3\beta\xi + 6\epsilon)}{2h(3\epsilon + \sigma\xi(h-\xi))}$$

Since $\int_K g_1\,dx \geq 0$, the second term on the right hand side of (24) attains its minimum if both $\int_{K_1} g_1\,dx$ and $\int_{K_2\cup K_3} g_1\,dx$ are positive. For sufficiently large σ, this is only possible if

$$\xi \leq \frac{3\beta + \sqrt{9\beta^2 + 24\epsilon\sigma}}{2\sigma} \tag{28}$$

On the other hand, we note that the first term on the right hand side of (24) is a locally decreasing function of ξ, since

$$\int_K |-\epsilon B_1^{*\prime\prime}|\,dx = -\alpha_1\frac{\epsilon h}{\xi(h-\xi)}$$

and

$$\frac{d}{d\xi}\left(-\alpha_1 \frac{\epsilon h}{\xi(h-\xi)}\right) = -\frac{\epsilon(h-2\xi)(-3\beta+2\sigma h-\sigma\xi))}{2\xi(h-\xi)(3\epsilon+\sigma\xi(h-\xi))} < 0 \tag{29}$$

for $\sigma h > 3\beta$. This fact together with (28) determines the optimal value ξ_e. □

Remark 3 The value of ξ_e coincides with the one suggested in [8].

Remark 4 The value of α_1 at ξ_e is simply equal to $\frac{\xi_e}{h} - 1$.

Hence we take $\eta = \eta_e$, $\xi = \min\{h - 2\eta, \xi_e\}$ and δ is chosen accordingly (i.e. $\delta = h - \eta - \xi$). We note that the points continuously get through from one regime to another in all cases.

Finally we recall that the pseudo bubble functions B_i^* $(i = 1, 2)$ are approximations to B_i on the sub-grid specified above, through (12) and they are used in place of B_i to represent u_B in (11). The approximate representation of u_B by bubble functions B_i^* $(i = 1, 2)$ is eventually used to solve (7) for its linear part.

4 Numerical results

In this section, we report some numerical experiments to illustrate the performance of the present algorithm in the interesting case of small diffusion which corresponds to the convection-dominated or reaction-dominated regimes depending on the ratio between the related problem parameters. We remark that the linear part of the numerical solution u_L only are presented in all figures.

Experiment 1: We first consider the constant-coefficient case where $\beta = 1$ and $f(x) = 1$. We compute the approximate solution on both uniform and non-uniform meshes. The uniform mesh is generated by dividing the unit interval $[0, 1]$ into ten elements, i.e., the mesh size $h = 1/10$ and the grid points $x_i = ih$ where $i = 0, 1, \ldots, 10$. The non-uniform mesh is randomly generated from the uniform mesh by adding a small fraction of h to x_i, so that the grid point x_i of the uniform mesh is replaced by a point between $x_i - \frac{h}{4}$ and $x_i + \frac{h}{4}$. We display the numerical results on the non-uniform mesh only because the results on the uniform mesh are similar, yet better. In Fig. 3, we present the linear part of the numerical solution u_L together with the exact solution u for $\epsilon = 10^{-2}$ and various intensities of reaction ($\sigma = 0.1, 1, 10, 20, 50, 100$). The corresponding numerical results for $\epsilon = 10^{-5}$ are reported in Fig. 4.

Experiment 2: We turn our attention to a variable-coefficient case for the same range of the problem parameters. We set $\beta = \frac{x+1}{6}$ and decompose the domain into a uniform discretization of 20 elements. Two different source functions are tested and the numerical results are displayed in Figs. 5, 6, 7, 8.

Experiment 3: We consider a more interesting variable-coefficient case which also exhibits an internal layer. We set $\beta = -2(2x - 1)$ and $f(x) = 4(2x - 1)$ and we decompose the domain into a uniform discretization of 25 elements. We report the corresponding numerical results in Figs. 9, 10.

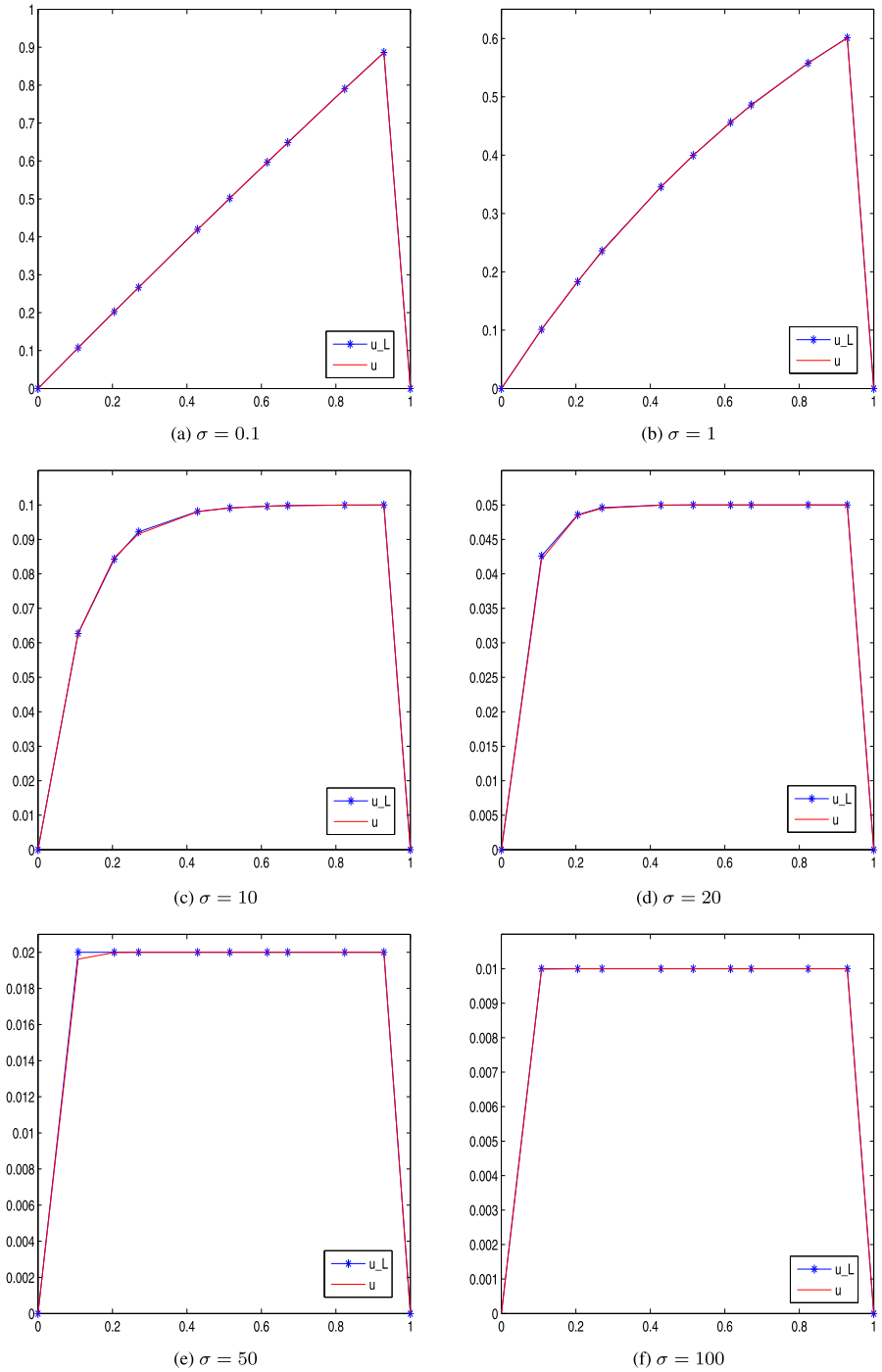

(a) $\sigma = 0.1$ (b) $\sigma = 1$

(c) $\sigma = 10$ (d) $\sigma = 20$

(e) $\sigma = 50$ (f) $\sigma = 100$

Fig. 3 The linear part u_L of the numerical solution and the exact solution u for several values of σ when $f(x) = 1$ and $\epsilon = 10^{-2}$

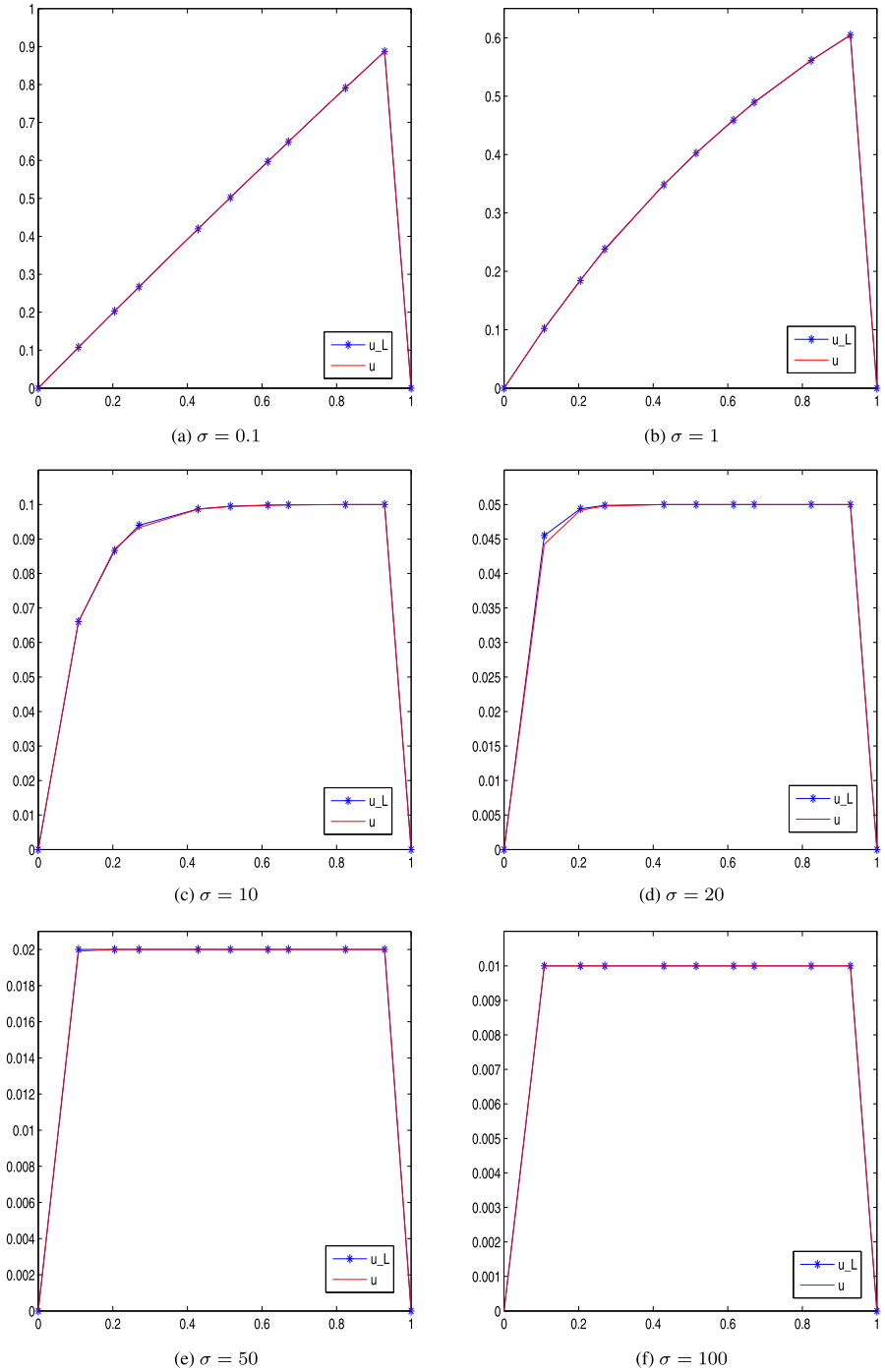

(a) $\sigma = 0.1$ (b) $\sigma = 1$

(c) $\sigma = 10$ (d) $\sigma = 20$

(e) $\sigma = 50$ (f) $\sigma = 100$

Fig. 4 The linear part u_L of the numerical solution and the exact solution u for several values of σ when $f(x) = 1$ and $\epsilon = 10^{-5}$

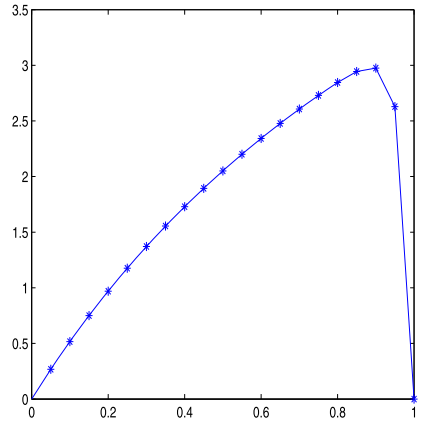

(a) $\sigma = 0.1$

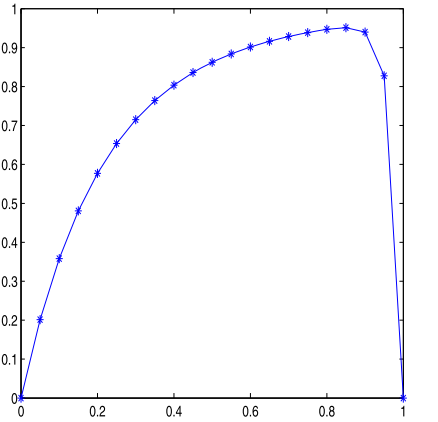

(b) $\sigma = 1$

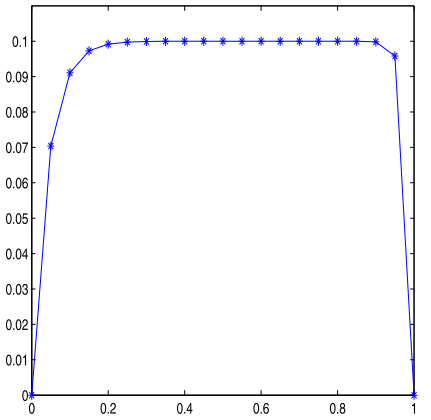

(c) $\sigma = 10$

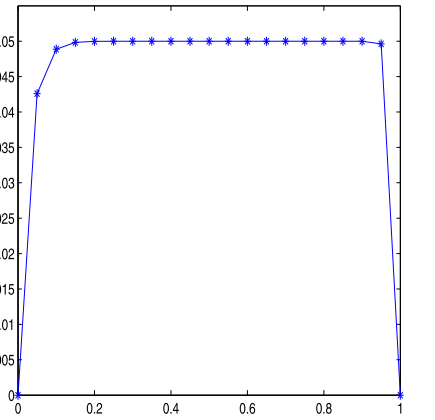

(d) $\sigma = 20$

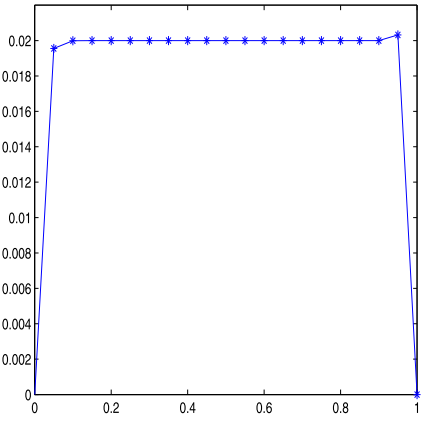

(e) $\sigma = 50$

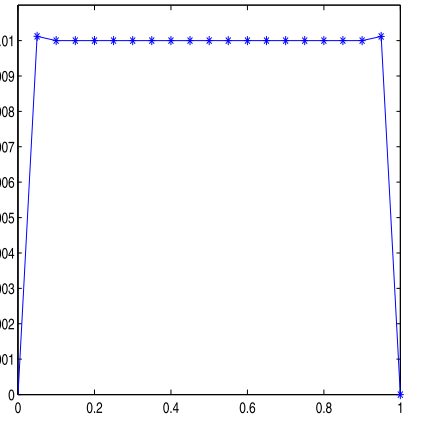

(f) $\sigma = 100$

Fig. 5 The linear part u_L of the numerical solution for several values of σ when $f(x) = 1$, $\epsilon = 10^{-2}$ and $\beta = \frac{x+1}{6}$

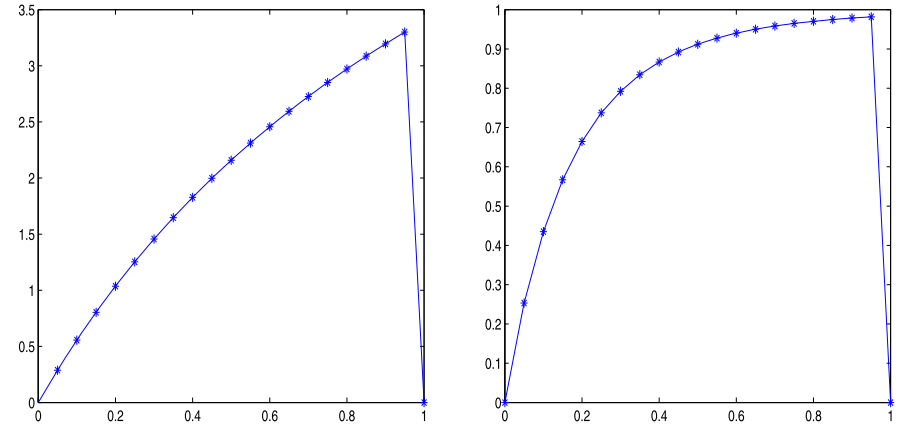

(a) $\sigma = 0.1$

(b) $\sigma = 1$

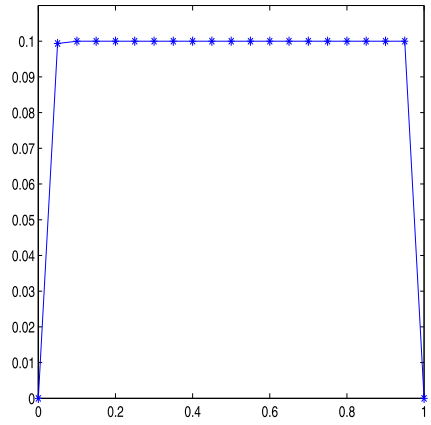

(c) $\sigma = 10$

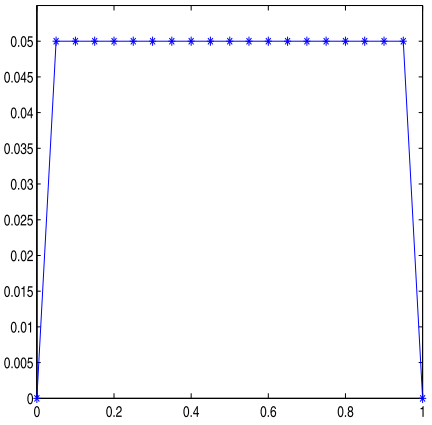

(d) $\sigma = 20$

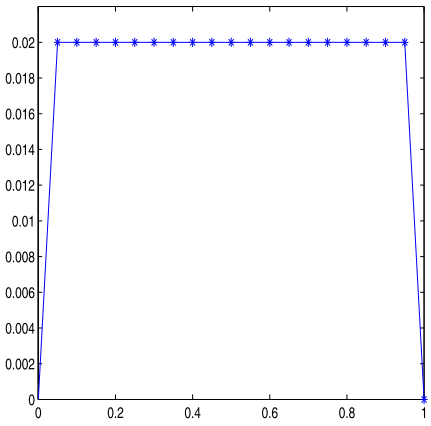

(e) $\sigma = 50$

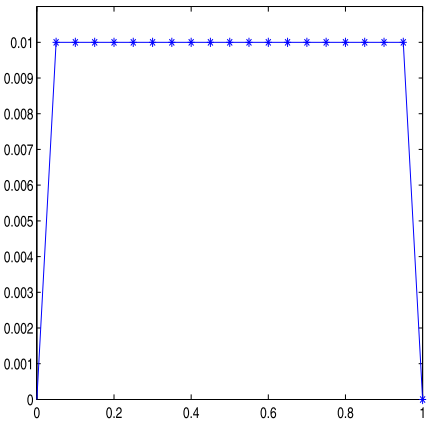

(f) $\sigma = 100$

Fig. 6 The linear part u_L of the numerical solution for several values of σ when $f(x) = 1$, $\epsilon = 10^{-5}$ and $\beta = \frac{x+1}{6}$

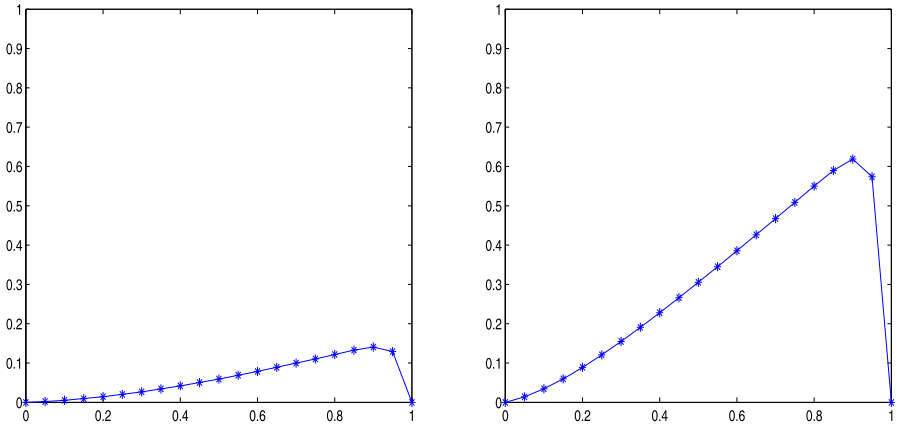

(a) $\sigma = 0.1$

(b) $\sigma = 1$

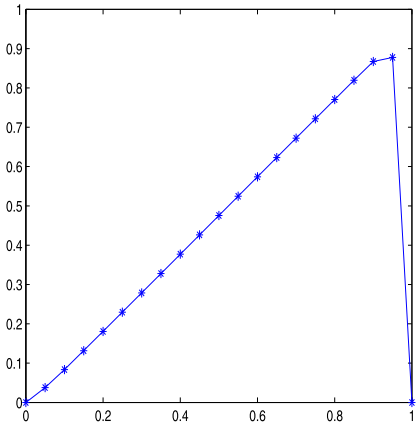

(c) $\sigma = 10$

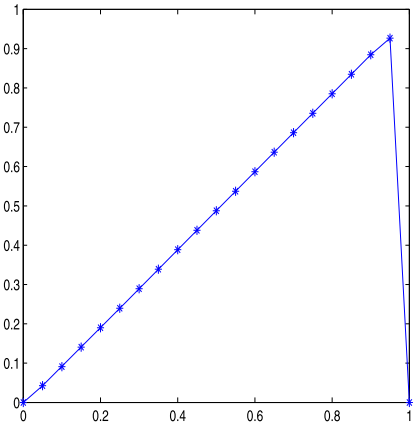

(d) $\sigma = 20$

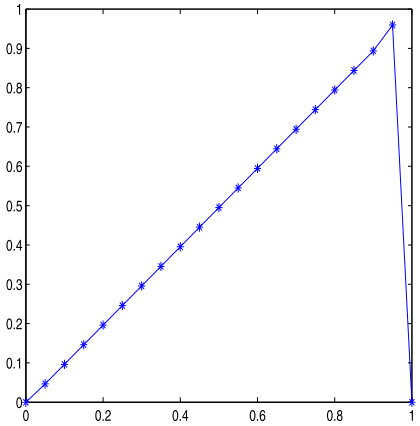

(e) $\sigma = 50$

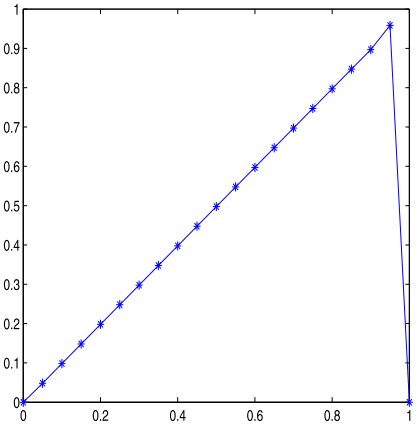

(f) $\sigma = 100$

Fig. 7 The linear part u_L of the numerical solution for several values of σ when $f(x) = \sigma x$, $\epsilon = 10^{-2}$ and $\beta = \frac{x+1}{6}$

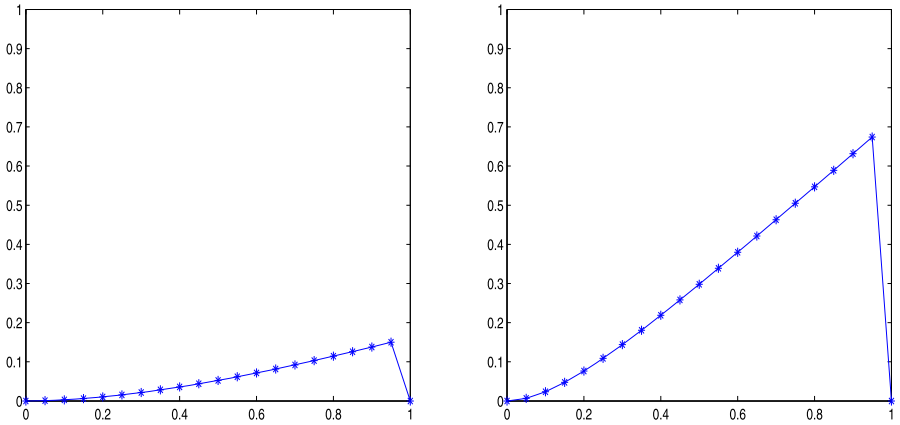

(a) $\sigma = 0.1$

(b) $\sigma = 1$

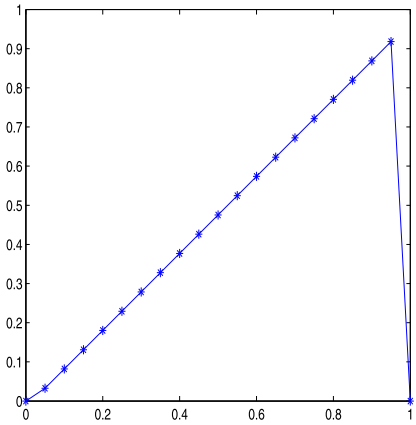

(c) $\sigma = 10$

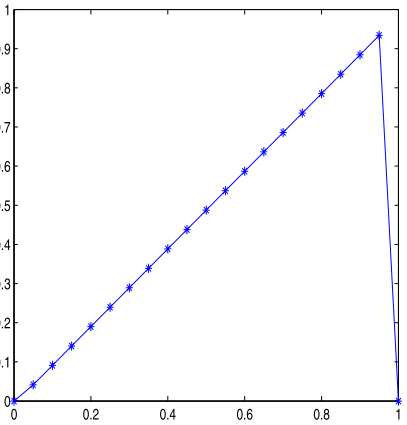

(d) $\sigma = 20$

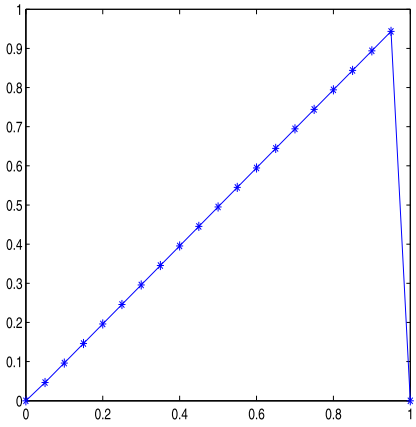

(e) $\sigma = 50$

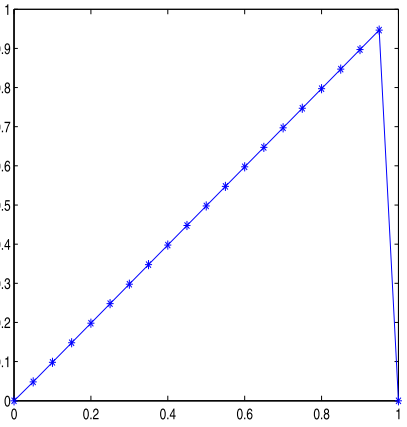

(f) $\sigma = 100$

Fig. 8 The linear part u_L of the numerical solution for several values of σ when $f(x) = \sigma x$, $\epsilon = 10^{-5}$ and $\beta = \frac{x+1}{6}$

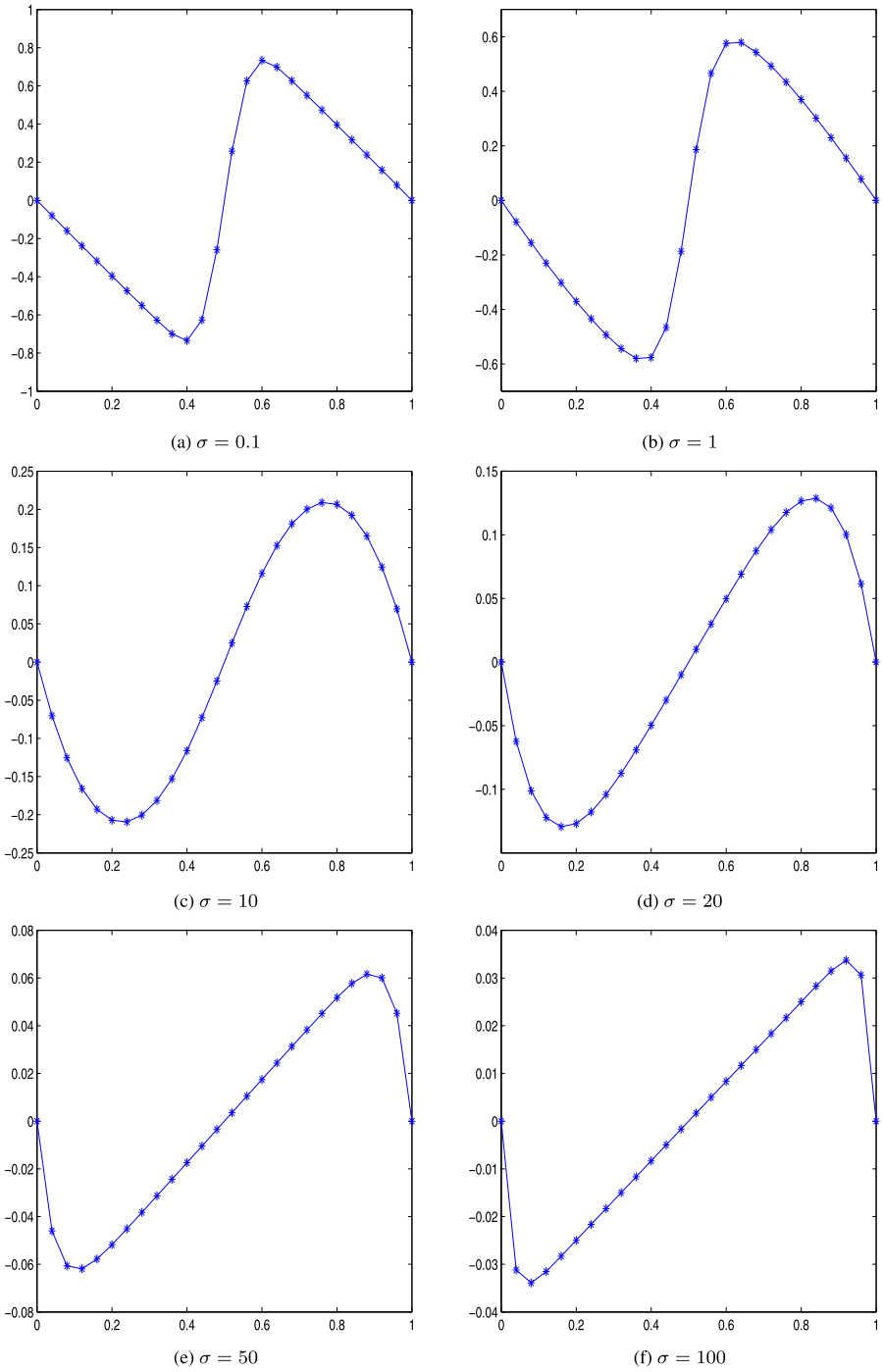

(a) $\sigma = 0.1$ (b) $\sigma = 1$

(c) $\sigma = 10$ (d) $\sigma = 20$

(e) $\sigma = 50$ (f) $\sigma = 100$

Fig. 9 The linear part u_L of the numerical solution for several values of σ when $f(x) = 4(2x - 1)$, $\epsilon = 10^{-2}$ and $\beta = -2(2x - 1)$

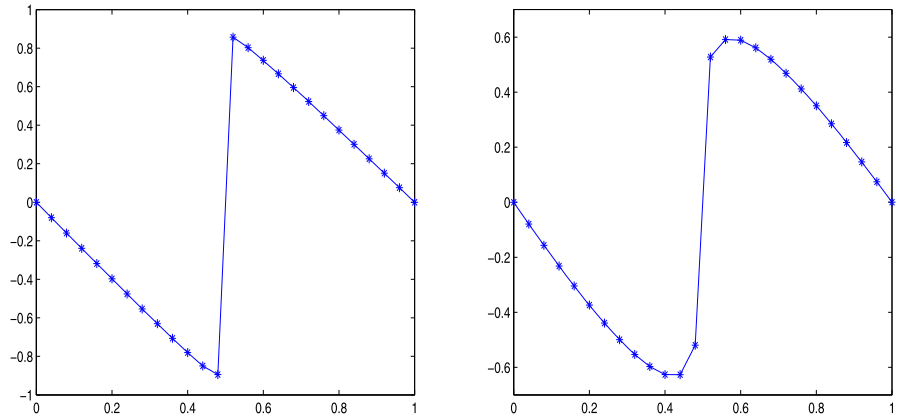

(a) $\sigma = 0.1$

(b) $\sigma = 1$

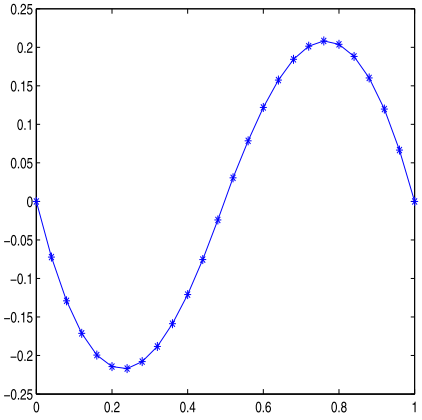

(c) $\sigma = 10$

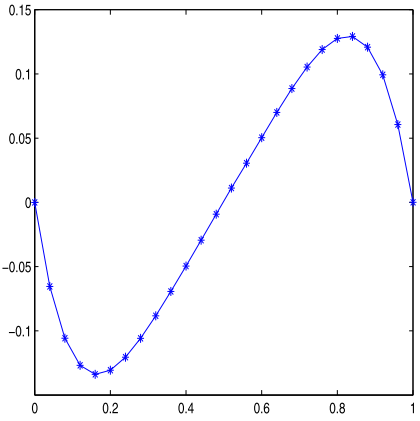

(d) $\sigma = 20$

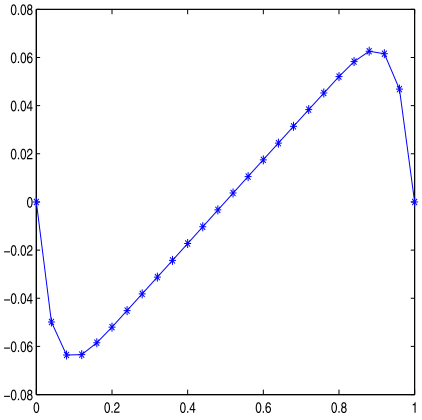

(e) $\sigma = 50$

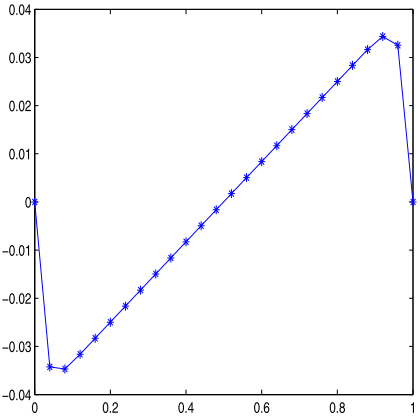

(f) $\sigma = 100$

Fig. 10 The linear part u_L of the numerical solution for several values of σ when $f(x) = 4(2x - 1)$, $\epsilon = 10^{-5}$ and $\beta = -2(2x - 1)$

In all three experiments, we report that the numerical results are in good agreement with the physical configuration of the problem for a wide range of parameters, even when the mesh is coarse. The transition from one regime to another is accurately captured by the algorithm. The related results are also comparable with the one in [8]. Therefore we may conclude that the pseudo RFBs retain the stability features of RFBs and provide us a robust, yet a cheap numerical method.

References

1. Baiocchi, C., Brezzi, F., Franca, L.P.: Virtual bubbles and the GaLS. Comput. Methods Appl. Mech. Eng. **105**, 125–141 (1993)
2. Brezzi, F., Bristeau, M.O., Franca, L.P., Mallet, M., Roge, G.: A relationship between stabilized finite element methods and the Galerkin method with bubble functions. Comput. Methods Appl. Mech. Eng. **96**, 117–129 (1992)
3. Brezzi, F., Russo, A.: Choosing bubbles for advection-diffusion problems. Math. Models Methods Appl. Sci. **4**, 571–587 (1994)
4. Brezzi, F., Marini, D., Russo, A.: Applications of pseudo residual-free bubbles to the stabilization of convection-diffusion problems. Comput. Methods Appl. Mech. Eng. **166**, 51–63 (1998)
5. Brezzi, F., Franca, L.P., Russo, A.: Further considerations on residual-free bubbles for advective-diffusive equations. Comput. Methods Appl. Mech. Eng. **166**, 25–33 (1998)
6. Brezzi, F., Marini, D., Süli, E.: Residual-free bubbles for advection-diffusion problems: The general error analysis. Numer. Math. **85**, 31–47 (2000)
7. Brezzi, F., Marini, D.: Augmented spaces, two-level methods, and stabilizing sub-grids. Int. J. Numer. Methods Fluids **40**, 31–46 (2002)
8. Brezzi, F., Hauke, G., Marini, D., Sangalli, G.: Link-cutting bubbles for the stabilization of convection-diffusion-reaction problems. Math. Models Methods Appl. Sci. **13**, 445–461 (2003)
9. Brezzi, F., Marini, D., Russo, A.: On the choice of a stabilizing subgrid for convection–diffusion problems. Comput. Methods Appl. Mech. Eng. **194**, 127–148 (2005)
10. Brooks, A.N., Hughes, T.J.R.: Streamline upwind/Petrov-Galerkin formulations for convection-dominated flows with particular emphasis on the incompressible Navier-Stokes equations. Comput. Methods Appl. Mech. Eng. **32**, 199–259 (1982)
11. Farrell, P.A., Hegarty, A.F., Miller, J.J.H., O'Riordan, E., Shishkin, G.I.: Robust computational techniques for boundary layers. Appl. Math. **16** (2000)
12. Franca, L.P., Frey, S.L., Hughes, T.J.R.: Stabilized finite element methods: I. Application to the advective-diffusive model. Comput. Methods Appl. Mech. Eng. **95**, 253–276 (1992)
13. Franca, L.P., Russo, A.: Deriving upwinding, mass lumping and selective reduced integration by RFB. Appl. Math. Lett. **9**, 83–88 (1996)
14. Franca, L.P., Nesliturk, A.I., Stynes, M.: On the stability of RFB for convection-diffusion problems and their approximation by a two-level FEM. Comput. Methods Appl. Mech. Eng. **166**, 35–49 (1998)
15. Franca, L.P., Tobiska, L.: Stability of the residual free bubble method for bilinear finite elements on rectangular grids. IMA J. Numer. Anal. **22**, 73–87 (2002)
16. Hughes, T.J.R., Franca, L.P., Hulbert, G.: A new finite element formulation for computational fluid dynamics: VIII. The Galerkin/least-squares method for advective-diffusive equations. Comput. Methods Appl. Mech. Eng. **73**, 173–189 (1989)
17. Nesliturk, A.I.: A stabilizing subgrid for convection-diffusion problem. Math. Models Methods Appl. Sci. **16**, 211–232 (2006)
18. Nesliturk, A.I.: On the choice of stabilizing subgrid for convection-diffusion problem on rectangular grids. Comput. Math. Appl. **59**, 3687–3699 (2010)
19. Sangalli, G.: Global and local error analysis for the residual-free bubbles method applied to advection-dominated problems. SIAM J. Numer. Anal. **38**, 1496–1522 (2000)